Research Article | Vol. 9, No. 6 | 1 Jun 2018 | BIOMEDICAL OPTICS EXPRESS 2755
Biomedical Optics EXPRESS

Dextran adsorption onto red blood cells revisited: single cell quantification by laser tweezers combined with microfluidics

KISUNG LEE,[1,2,3,8] EVGENY SHIRSHIN,[2,8] NATALIYA ROVNYAGINA,[2] FRANCOIS YAYA,[1,4] ZAKARIA BOUJJA,[1,5] ALEXANDER PRIEZZHEV,[2,6] AND CHRISTIAN WAGNER[1,7,*]

[1]*Experimental Physics, Saarland University, Saarbrücken, D-66041, Germany*
[2]*Faculty of Physics, Lomonosov Moscow State University, Moscow, 119991, Russia*
[3]*Curremtly with Ulsan National Institute of Science and Technology, Institute for Basic Science, Center for Soft and Living Matter, Ulsan, 44919, South Korea*
[4]*Laboratoire Interdisciplinaire de Physique, UMR 5588 CNRS and University Grenoble–Alpes, Saint Martin d'Hères Cedex, B.P. 87, 38402, France*
[5]*LaMCScI, University Mohamed V, Faculty of Sciences, Rabat, Morocco*
[6]*International Laser Center, Lomonosov Moscow State University, Moscow, 119991, Russia*
[7]*Physics and Materials Science Research Unit, University of Luxembourg, L-1511, Luxembourg*
[8]*Co-first authors with equal contribution*
[*]*c.wagner@mx.uni-saarland.de*

Abstract: The aggregation of red blood cells (RBC) is of importance for hemorheology, while its mechanism remains debatable. The key question is the role of the adsorption of macromolecules on RBC membranes, which may act as "bridges" between cells. It is especially important that dextran is considered to induce "bridge"-less aggregation due to the depletion forces. We revisit the dextran-RBC interaction on the single cell level using the laser tweezers combined with microfluidic technology and fluorescence microscopy. An immediate sorption of ~10^4 molecules of 70 kDa dextran per cell was observed. During the incubation of RBC with dextran, a gradual tenfold increase of adsorption was found, accompanied by a moderate change in the RBC deformability. The obtained data demonstrate that dextran sorption and incubation-induced changes of the membrane properties must be considered when studying RBC aggregation *in vitro*.

OCIS codes: (170.1530) Cell analysis; (020.7010) Laser trapping; (170.2520) Fluorescence microscopy.

References and links

1. O. K. Baskurt and H. J. Meiselman, "Blood rheology and hemodynamics," Semin. Thromb. Hemost. **29**(5), 435–450 (2003).
2. M. Girasole, G. Pompeo, A. Cricenti, G. Longo, G. Boumis, A. Bellelli, and S. Amiconi, "The how, when, and why of the aging signals appearing on the human erythrocyte membrane: an atomic force microscopy study of surface roughness," Nanomedicine (Lond.) **6**(6), 760–768 (2010).
3. O. Baskurt, B. Neu, and H. J. Meiselman, *Red Blood Cell Aggregation* (CRC Press, 2012).
4. V. Schechner, I. Shapira, S. Berliner, D. Comaneshter, T. Hershcovici, J. Orlin, D. Zeltser, M. Rozenblat, K. Lachmi, M. Hirsch, and Y. Beigel, "Significant dominance of fibrinogen over immunoglobulins, C-reactive protein, cholesterol and triglycerides in maintaining increased red blood cell adhesiveness/aggregation in the peripheral venous blood: a model in hypercholesterolaemic patients," Eur. J. Clin. Invest. **33**(11), 955–961 (2003).
5. D. Lominadze and W. L. Dean, "Involvement of fibrinogen specific binding in erythrocyte aggregation," FEBS Lett. **517**(1-3), 41–44 (2002).
6. S. Chien and K. M. Jan, "Surface adsorption of dextrans on human red cell membrane," J. Colloid Interface Sci. **62**(3), 461–470 (1977).
7. A. Pribush, D. Zilberman-Kravits, and N. Meyerstein, "The mechanism of the dextran-induced red blood cell aggregation," Eur. Biophys. J. **36**(2), 85–94 (2007).
8. S. Chien and K. Jan, "Ultrastructural basis of the mechanism of rouleaux formation," Microvasc. Res. **5**(2), 155–166 (1973).

#324551 https://doi.org/10.1364/BOE.9.002755
Journal © 2018 Received 20 Feb 2018; revised 28 Apr 2018; accepted 6 May 2018; published 22 May 2018

Biomedical Optics EXPRESS

9. P. J. Bronkhorst, J. Grimbergen, G. J. Brakenhoff, R. M. Heethaar, and J. J. Sixma, "The mechanism of red cell (dis)aggregation investigated by means of direct cell manipulation using multiple optical trapping," Br. J. Haematol. **96**(2), 256–258 (1997).
10. K. Lee, C. Wagner, and A. V. Priezzhev, "Assessment of the "cross-bridge"-induced interaction of red blood cells by optical trapping combined with microfluidics," J. Biomed. Opt. **22**(9), 091516 (2017).
11. B. Neu, R. Wenby, and H. J. Meiselman, "Effects of dextran molecular weight on red blood cell aggregation," Biophys. J. **95**(6), 3059–3065 (2008).
12. S. Chien, L. A. Sung, S. Kim, A. M. Burke, and S. Usami, "Determination of aggregation force in rouleaux by fluid mechanical technique," Microvasc. Res. **13**(3), 327–333 (1977).
13. A. Cudd, T. Arvinte, B. Schulz, and C. Nicolau, "Dextran protection of erythrocytes from low-pH-induced hemolysis," FEBS Lett. **250**(2), 293–296 (1989).
14. D. E. Brooks, "The effect of neutral polymers on the electrokinetic potential of cells and other charged particles: III. Experimental studies on the dextran/erythrocyte system," J. Colloid Interface Sci. **43**(3), 700–713 (1973).
15. F. J. Alvarez, A. Herráez, M. C. Tejedor, and J. C. Díez, "Behaviour of isolated rat and human red blood cells upon hypotonic-dialysis encapsulation of carbonic anhydrase and dextran," Biotechnol. Appl. Biochem. **23**(Pt 2), 173–179 (1996).
16. K. Fricke, K. Wirthensohn, R. Laxhuber, and E. Sackmann, "Flicker spectroscopy of erythrocytes. A sensitive method to study subtle changes of membrane bending stiffness," Eur. Biophys. J. **14**(2), 67–81 (1986).
17. J. Janzen and D. E. Brooks, "A critical reevaluation of the nonspecific adsorption of plasma proteins and dextrans to erythrocytes and the role of these in rouleaux formation," in *Interfacial Phenomena in Biological Systems*, M. Bender, ed. (Marcel Dekker 1991).
18. M. W. Rampling, "Red cell aggregation and yield stress," in *Clinical Blood Rheology*, G.D.O.Lowe, ed. (CRC Press 1988).
19. P. Steffen, C. Verdier, and C. Wagner, "Quantification of depletion-induced adhesion of red blood cells," Phys. Rev. Lett. **110**(1), 018102 (2013).
20. H. Bäumler, B. Neu, S. Iovtchev, A. Budde, H. Kiesewetter, R. Latza, and E. Donath, "Electroosmosis and polymer depletion layers near surface conducting particles are detectable by low frequency electrorotation," Colloids Surf. A Physicochem. Eng. Asp. **149**(1), 389–396 (1999).
21. H. Bäumler, B. Neu, R. Mitlöhner, R. Georgieva, H. J. Meiselman, and H. Kiesewetter, "Electrophoretic and aggregation behavior of bovine, horse and human red blood cells in plasma and in polymer solutions," Biorheology **38**(1), 39–51 (2001).
22. S. Rad, H. J. Meiselman, and B. Neu, "Impact of glycocalyx structure on red cell-red cell affinity in polymer suspensions," Colloids Surf. B Biointerfaces **123**, 106–113 (2014).
23. B. Neu and H. J. Meiselman, "Depletion-Mediated Red Blood Cell Aggregation in Polymer Solutions," Biophys. J. **83**(5), 2482–2490 (2002).
24. S. Shin, J.X. Hou, and M. Singh, "Validation and application of a microfluidic ektacytometer (RheoScan-D) in measuring erythrocyte deformability," Clin. Hemorheol. Microcirc. **37**, 319–328 (2007).
25. M. W. Rampling, H. J. Meiselman, B. Neu, and O. K. Baskurt, "Influence of cell-specific factors on red blood cell aggregation," Biorheology **41**(2), 91–112 (2004).
26. R. I. Weed, P. L. LaCelle, and E. W. Merrill, "Metabolic dependence of red cell deformability," J. Clin. Invest. **48**(5), 795–809 (1969).
27. M. Uyuklu, M. Cengiz, P. Ulker, T. Hever, J. Tripette, P. Connes, N. Nemeth, H. J. Meiselman, and O. K. Baskurt, "Effects of storage duration and temperature of human blood on red cell deformability and aggregation," Clin. Hemorheol. Microcirc. **41**(4), 269–278 (2009).
28. T. Betz, M. Lenz, J. F. Joanny, and C. Sykes, "ATP-dependent mechanics of red blood cells," Proc. Natl. Acad. Sci. U.S.A. **106**(36), 15320–15325 (2009).
29. N. Mohandas and S. B. Shohet, "The role of membrane-associated enzymes in regulation of erythrocyte shape and deformability," Clin. Haematol. **10**(1), 223–237 (1981).
30. A. Makhro, R. Huisjes, L. P. Verhagen, M. M. Mañú-Pereira, E. Llaudet-Planas, P. Petkova-Kirova, J. Wang, H. Eichler, A. Bogdanova, R. van Wijk, J.-L. Vives-Corrons, and L. Kaestner, "Red Cell Properties after Different Modes of Blood Transportation," Front. Physiol. **7**, 288 (2016).
31. K. J. A. Davies and A. L. Goldberg, "Proteins damaged by oxygen radicals are rapidly degraded in extracts of red blood cells," J. Biol. Chem. **262**(17), 8227–8234 (1987).
32. J. C. A. Cluitmans, M. R. Hardeman, S. Dinkla, R. Brock, and G. J. C. G. M. Bosman, "Red blood cell deformability during storage: towards functional proteomics and metabolomics in the Blood Bank," Blood Transfus. **10**(2), s12–s18 (2012).

1. Introduction

RBC properties such as deformability and aggregation propensity are the key factors governing microrheological properties of blood [1]. At low shear rates, the reversible formation of aggregates determines blood viscosity and flow resistance, affecting many aspects of *in vivo* hemodynamics [2-3]. This process is of interest for clinical applications as well as important for fundamental understanding of cellular interaction mechanisms.

Biomedical Optics EXPRESS

In vivo, the interaction between RBC is mediated by external proteins, which are present in blood plasma, such as albumin, gamma-globulin, fibrinogen etc [4]. Some of these proteins, e.g. fibrinogen, may adsorb on the membrane surface by either non-specific or specific binding [5], and it is sometimes assumed that molecular "bridging", i.e. formation of intercellular bonds via adsorbed molecules, is responsible for RBC aggregation [6–10]. The other point of view is that the role of blood plasma proteins in RBC aggregation is due to the formation of depletion layers between the adjacent cells leading to their attraction caused by osmotic pressure [3,11]. Elucidation of the RBC interaction mechanism in such a multicomponent system as blood plasma is complicated, and thus led to numerous studies of model systems with controlled parameters. Hence, RBC interaction is widely studied in model solutions of polymers, such as dextrans with different molecular weights, which may induce the formation of RBC aggregates. Surprisingly, in this case the mechanism of RBC interaction is also contradictive [6,7,11,12].

For dextran, its sorption on the RBC membrane has been studied for decades using various methods: electron microscopy [13], radiolabelling [6,14], fluorescent labelling [15], zeta-potential measurement [14] and flicker spectroscopy [16]. Being a neutral polymer, dextran molecules may penetrate into the glycocalyx and interact with phospholipids and carbohydrate groups on the external surface of the RBC membrane. For instance, Chien et al. [6] experimentally estimated that up to ~$9 \cdot 10^{-14}$ g of radio-labelled dextran 70 kDa can be adsorbed onto a single RBC. The authors conclude that the dextran-induced bridging of adjacent cells is responsible for RBCs aggregation. Cudd et al. [13] demonstrated that dextrans with molecular weight higher than 40 kDa (~4.5 nm Stokes radius) may efficiently protect RBC from low-pH-induced hemolysis by adsorbing and "covering" holes, which appear in the membrane. In their work, the defects in the membrane and dextran adsorption were visualized using electron microscopy. However, it is sometimes considered that RBC adsorption data for dextran, obtained in the early works, are subjected to potential artifacts and are difficult to interpret [17,18].

The other well-accepted hypothesis is that the formation of a depletion layer is responsible for RBC aggregation in the presence of dextran [10,19]. Based on the changes in dextran-induced electrophoretic mobility of RBC, it was suggested that the formation of depletion layers is the major process determining RBCs aggregation [11,20,21]. Nevertheless, even when considering the depletion layer formation to be the main effect responsible for cells aggregation, the fact of dextran adsorption is not excluded and the importance of taking it into account when modelling the cells interaction is mentioned [11,21,22], though it is not considered a necessary prerequisite for aggregation [18]. For instance, some authors consider that dextran penetrates into glycocalyx resulting in inhibition of depletion forces, and theoretical estimations predict a dramatic enhancement of cells interaction in the case if the penetration is lacking [23].

Hence, despite decades of investigation, the problem of quantification of dextran adsorption onto RBC membrane still remains challenging for a proper understanding of its role in the alteration of RBC properties and their interaction. Here we revisit the problem of dextran adsorption on RBC using an approach based on the laser tweezers technique coupled to the microfluidic platform and fluorescence microscopy. The developed method allows for quantifying the fluorescently labelled dextran adsorption on the level of individual cells and is therefore free of such potential artefacts as the trapped fluid [17], which may be significant when working with a suspension of cells. The time course of adsorption was followed for several hours to investigate the effect of possible alterations of the cells' intrinsic properties, which may occur due to RBC storage or interaction with dextran. Besides the significance of the results obtained for the particular field of microcirculation and blood rheology, RBC membrane is a model used for the studies of interactions of mammalian cell membranes with foreign molecules and their biocompatibility [19]. This fact makes the proposed method for quantification of polymer-RBC membrane interaction of a general significance.

Biomedical Optics EXPRESS

2. Materials and methods

2.1 Single cell level quantification of dextran adsorption on RBC: laser tweezers coupled to the microfluidic platform

The experimental setup used for quantifying the dextran adsorption onto a single RBC was similar to the one used in our previous work [10]. It is based on the inverted microscope (TE 2000, Nikon, Japan), and the schematic layout of the setup is shown in Fig. 1(A). Optical traps were formed using a laser beam from single-mode Nd:YAG laser (1064 nm, 1.5 W, Ventus 1064, Laser Quantum, UK) reflected by the parallel aligned nematic liquid crystal spatial light modulator (PAL-SLM, PPM X8267-15, Hamamatsu Photonics, Japan) and focused with a large numerical aperture oil immersion objective (N.A. 1.40, 60 × , Nikon, Japan). We used laser power up to 40 mW at the focal point. At the given wavelength and power, the heating of the sample can be considered negligible [24]. The positions of the traps were controlled independently in XYZ-plane within the focal plane of the objective using PAL-SLM. Visual control (in the reflection mode) of the trapped objects and detection of fluorescence intensity of the sample was performed in a transmission configuration using the CMOS camera (ORCA Flash 4.0 V3, Hamamatsu, Japan). When measuring fluorescence signal, the exposure time was set to 33 ms, and 4×4 binning of the images was used. The fluorescence excitation and registration was performed using a mercury lamp (HB-10103AF, Nikon, Japan) and FITC dichroic cube (fluorescein isothiocyanate-filter, Nikon, Japan) with a 480/30 nm excitation and 535/45 nm emission bands, correspondingly. Two values of excitation intensity were used: I_0 ~5 mW, when no filter was used, and I_0/24, when the ND filter was installed. When measuring the fluorescence signal from the dextran molecules adsorbed on RBC, excitation intensity was set to I_0, if not mentioned otherwise. In the case of calibration measurements with fluorescence beads excitation intensity was set to I_0/24. Microfluidic flow control system (MK-1, Elveflow, France) was used to pump the samples through the microfluidic device.

The sample preparation protocol was as follows: (1) fluorescent dextran solution (20 mg/ml, FITC-conjugated dextran 70 kDa, Sigma, catalog no. 46945) was prepared in phosphate buffered saline (PBS, pH 7.4, 290 mOsm, Invitrogen); (2) blood was taken by fingerpick method and a small amount was added to the dextran solution to achieve the final concentration of RBC ~0.05%; (3) the suspension was incubated at 22°C for a certain period of time and used for the measurements. For the experiments with pre-incubation, the cells were kept in PBS for 120 minutes, and then re-suspended in the fluorescent dextran solution followed by additional incubation for a given period of time.

The experimental cuvette consisted of a chamber connected to a microchannel (Fig. 1(B)). The chamber was much larger (3×2×0.5 cm) than the microchannel (100×40×30 μm), which was connected to a micro-pump and used to maintain two different solutions. The microchannel chip was made based on PDMS (Polydimethylsiloxane), and attached to the borosilicate cover glass. The larger chamber was also covered with a cover glass to avoid evaporation. Gentle flushing of a solution from the microchannel towards the chamber allowed for maintaining two different solutions. Due to the significant difference in the volumes, we could neglect the changes of the solution in the chamber. The microchannel was initially filled up with PBS solution (S2), afterwards 200 μL of RBC suspension in fluorescent dextran solution was put into the chamber (S1). The diffusion was prevented by continuously flushing S2 towards S1 at flow velocity v_{flush} = 20 μm/s. Test measurements have shown that at the given v_{flush} the diffusion does not take place for at least 30 minutes and the fluorescent signal in S2 remains almost at the level of noise.

In order to measure the adsorption of dextran, we trapped a single RBC with the laser tweezer, and lifted it up by 15 μm relative to the surface, and quickly transferred it from the larger chamber into the microchannel (see Visualization 1, Fig. 1(B)). Then, the fluorescence signal was recorded as shown in Fig. 1(B). Typical transition time was below 1 minute. To

Biomedical Optics EXPRESS

minimize the discrepancy in fluorescence intensity signal caused by changes in absorption/scattering due to changes in the cell geometry, laser power was kept constant (30 mW) to ensure similarity of RBC shape in the optical trap.

To ensure that the observed RBC fluorescence is due to the adsorption of dextran, but not due to the FITC detachment from dextran macromolecule and its adsorption on RBCs, we performed an additional test using 3 kDa filtration and size-exclusion chromatography, and confirmed that there is no FITC desorption from dextran, at least on the time scale of a typical experiment. FITC-conjugated dextran 70 kDa (Sigma, catalog no. 46945) was used in the adsorption experiments. Previously to the measurements, we verified the absence of free FITC in dextran solution and the absence of FITC desorption from dextran with time. For this, 3 kDa centrifugal filter (Amicon Ultra, Sigma) was used. The solution of fluorescently labeled 70 kDa dextran (20 mg/ml in PBS) was filtered through a 3 kDa membrane, and fluorescence of the solution after filtration was measured. It was observed that only the part of solution, which did not pass through the membrane, exhibited fluorescence, thus confirming the absence of free or desorbed FITC in the system.

For the calibration measurements 2 μm fluorescent red carboxylate-modified polystyrene latex beads (Sigma, catalog no. L3030) were used. To measure the z-profile of the fluorescence detection volume, the bead was moved stepwise in the vertical plane using the PAL-SLM without moving the objective, i.e. the parameters of excitation and detection were kept constant. Positioning of the trap to the center of the excitation beam was performed using the coordinates of the point with maximum fluorescence intensity obtained in the experiments with dextran solution. The error was taken as standard deviation calculated from three independent measurements. Fluorescence intensity was calculated as the average over the 25% of points with the highest intensity.

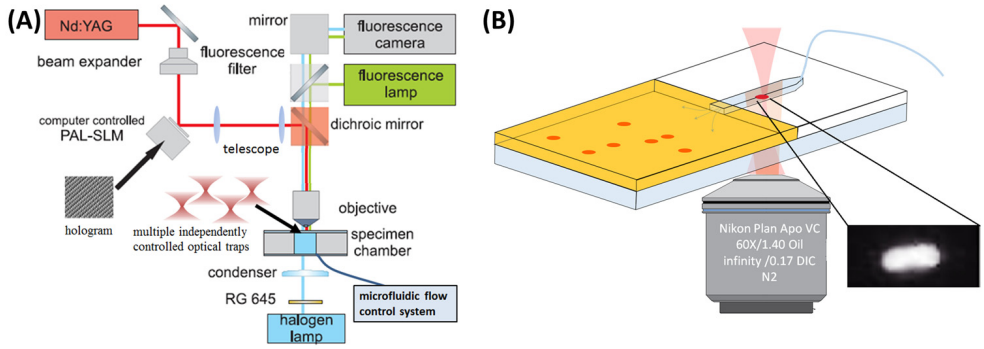

Fig. 1. (A) Schematic layout of the holographic laser tweezer combined with microfluidic chip and fluorescence microscopy for measuring the dextran adsorption on RBC. See text for details. (B) Sketch of the experimental chamber used for the measurement of dextran adsorption on RBC (not in scale). The larger chamber contained the fluorescent dextran solution (shown in yellow) and the microchannel was filled with PBS (shown in blue). Gentle flushing (indicated with blue arrows) prevented the diffusion of solutions. The inset shows the fluorescence image obtained from the cell trapped in the chamber and moved to the microchannel with PBS (see Visualization 1 for the transition procedure).

2.2 Ektacytometry measurements

Ektacytometry measurements were performed to follow up the time course of changes in RBC properties (namely, deformability of the cells) that could accompany the RBC incubation in dextran solution. The measurements were performed using a commercial laser ektacytometer (RheoScan AnD-300, RheoMeditech, Korea) that measures the RBC deformability index (DI), a common parameter used in clinical hemorheology [24].

The sample preparation protocol was as follows: (1) 70 kDa dextran (Pharmacia Biotech, Sweden) solution in PBS was prepared; (2) whole blood was taken by fingerpick method and

Biomedical Optics EXPRESS

a small amount was added to the dextran solution to achieve the final concentration of RBC ~1%; (3) the suspension was incubated at the room temperature (22°C) for a certain period (0-180 minutes); (4) after incubation, the cells were gently centrifuged (300g, 5 minutes) and re-suspended in highly viscous (40 cP) polyvinylpyrrolidone solution to reach the cell concentration of 1%. The final solution was used for measuring the DI. For control measurements, to investigate RBC storage effect, the cells were incubated in PBS, instead of dextran solution.

A diluted suspension of RBC was put into a special chamber, where it was pressure driven and shear-elongated at 37°C. The dependence of RBC elongation on applied shear stress was measured by analyzing the diffraction patterns of the laser beam, passing through the suspension. According to the established algorithm, the isointensity levels of the diffraction patterns were approximated with ellipses, which elongation gradually shrinks along with decreasing shear stress. At certain levels of the latter, the DI was calculated as a ratio between the sum and difference of the longer and smaller axes of ellipse.

3. Results

3.1 The time course of dextran adsorption onto RBC

Figure 2 demonstrates the time course of normalized integral fluorescence intensity for cells moved to the channel with PBS. As RBC are essentially non-fluorescent under the excitation wavelength used (550 nm), the detected fluorescence signal from the cell area was indicative of dextran adsorption. After moving an individual RBC from the solution with fluorescent dextran to PBS, we could observe a significant fluorescence signal (see the insets in Fig. 2(A)). This process is illustrated in the Visualization 1.

As in the channel with PBS, desorption of dextran and photobleaching were observed, which occurred on the time scale of a minute (see Fig. 2(B) and 2(C); the fluorescence intensity values in Fig. 2(A) were taken as the maximum initial values.

The excitation intensity in Fig. 2(B) is 24 times higher compared to Fig. 2(C), while the corresponding decay times are 25 and 100 s. Considering the fact that the rate of photobleaching $k_{\text{bleaching}}$ is determined by the excitation intensity I (in the case of a single fluorophore $k_{\text{bleaching}} \sim I$), one can conclude that the decay of fluorescence intensity in Fig. 2(C) is mainly due to dextran desorption form the cell. Hence, the desorption rate was estimated as ~0.01 s^{-1}.

The kinetics of dextran adsorption was followed by measuring the incubation time dependence of fluorescence signal. For this purpose, RBC were sequentially moved to the channel with PBS, and the total times of cells incubation correspond to the values in the X-axis in Fig. 2(A). As a result, we observed that dextran adsorption increases gradually as a function of time (Fig. 2(A)).

To investigate the influence of RBC pretreatment, adsorption kinetics was measured after 2 and 4 hours of RBC preincubation in PBS. After preincubation, the cells were resuspended in the fluorescent dextran solution in the microfluidic chip, and the time course of fluorescence intensity was studied. In this case, after preincubation for 2 hours the initial signal was close to that in the absence of preincubation, but increased more rapidly with time. Longer preincubation (4 hours) also did not result in the immediate enhancement of signal.

Biomedical Optics EXPRESS

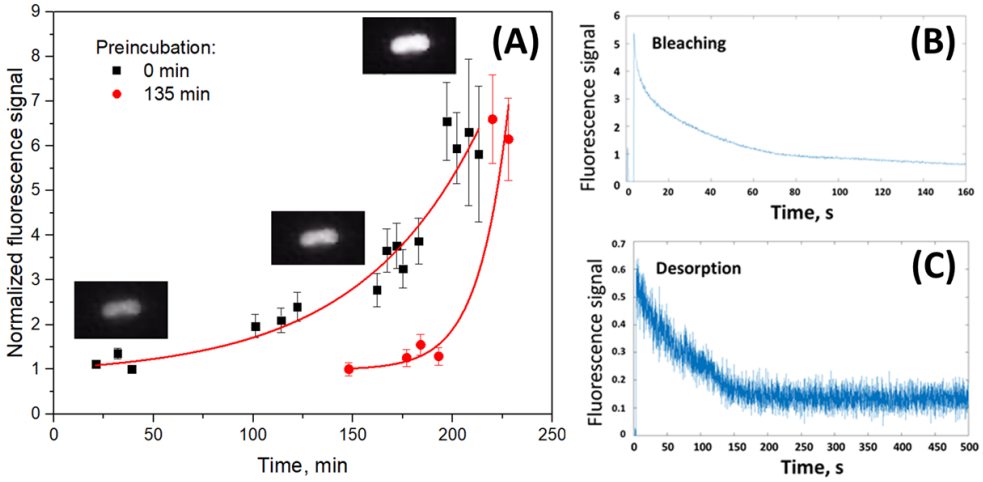

Fig. 2. (A) The dependence of maximum fluorescence intensity on incubation time: black and red dots correspond to 0 and 135 minutes of RBC preincubation in PBS respectively. The microphotographs in the insets illustrate changes in the fluorescence intensity detected in the channel with PBS. Here, fluorescence intensity was normalized to the value obtained in the first point. Intensity of excitation was kept same for all measurements shown in (A) and was roughly estimated as 5 mW at the sample. The error bars correspond to the averaging over three independent microchannels used in the experiment. (B) and (C) show the fluorescence decay kinetics of one cell obtained at two values of excitation intensities: I_0 ~5 mW (B), when no filter was used, and $I_0/24$ (C), when the ND filter was installed.

As the next step, we aimed at a quantitative estimation of the number of adsorbed molecules per cell. For this, the measurement of the fluorescence detection volume was performed with microbeads as described below.

3.2 Quantification of the number of adsorbed molecules

First, to obtain the calibration curve, the microchannel was filled with the solution of dextran at different concentrations and the fluorescence signal was recorded (Fig. 3(A)). To obtain the calibration curve, we used the following protocol: (1) Empty channel was filled with the solution of fluorescent dextran of different concentration; (2) Fluorescence signal of the sample was measured, and the initial (i.e. maximum) value was used for the calibration curve. The signal was averaged over the central area of the image with the highest intensity, and this area was selected similar for all concentrations; (3) For lower concentrations, exposition was increased, and the detected fluorescence signal was divided by the exposition enhancement (i.e. the intensities were normalized to the exposition); (4) After that, the dependence of fluorescence intensity on fluorophore concentration was plotted (see Fig. 3(A)).

To properly calculate the number of molecules, which contributed to the overall fluorescence signal, the geometry of the detection volume was assessed. For this purpose, the z-dependence of fluorescence intensity (i.e. the depth of field) was determined using 2 μm fluorescent beads. The bead was trapped and moved in the Z-direction in a stepwise manner relative to the focal plane of the objective. The measurements were performed in the microchannel filled with PBS. The position of the trap was changed by adjusting the PAL-SLM mask parameters while keeping the objective position constant, that allowed moving the trap relative to the excitation beam without changing the geometry of the latter in the sample (Fig. 3(B)). The fluorescent signal from the bead was strong enough to use low level excitation and avoid photobleaching within the time scales of the calibration procedure. The obtained dependence of fluorescence intensity on z-shift is shown in Fig. 3(C). We assumed that the excitation intensity is constant along the Z-axis in the detection volume and the obtained Z-profile is due to the depth of field profile of the optical system of the microscope.

Biomedical Optics EXPRESS

The lateral dimensions and beam profile distribution were obtained by processing the images of dextran solution fluorescence. Next, for the detection volume $V_{det} = 1.2 \cdot 10^5$ μm^3, that corresponds to ~10^9 dextran molecules at 10^{-3} mg/ml concentration, integral fluorescence intensity was calculated as a sum over the corresponding points of the image obtained for fluorescent dextran solution. When measuring fluorescence I_{RBC} from RBC, the trap is always kept in the center of the excitation beam close to the focal plane, i.e. in this case excitation intensity is set to the maximum value. In case of dextran solution, signal is detected from points with different excitation intensity and detection efficiency. Hence, to compare between the signals for RBC and solution, the integral intensity measured for solution was normalized to the X-Y and Z distributions of intensity. Finally, by comparing the normalized intensity value for a dextran solution with known concentration and RBC, the number of adsorbed molecules was estimated. This procedure yielded $2 \cdot 10^4$ dextran molecules adsorbed per a single RBC in the initial time point, reaching ~10^5 molecules after incubation (Fig. 2(A)). To estimate the sensitivity of our measurement system, the calibration curve (Fig. 3(A)) was fitted linearly, and its intercept with the Y-axis was obtained. This value corresponded to the signal from ca 100 molecules, hence, this value vas taken as a STD error (σ), and the detection limit was estimated as 3σ (~300 molecules).

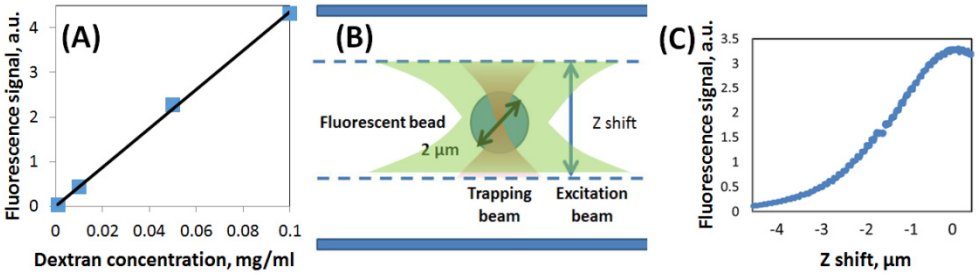

Fig. 3. (A) Dependence of the integral fluorescence intensity for the solution of dextran with different concentrations. (B) Schematic layout of the procedure used for measuring the fluorescence detection volume in the z-direction. A 2 μm fluorescent bead was moved with an optical trap using spatial light modulator, while the detection volume was fixed. (C) The dependence of bead's fluorescence intensity on z-shift. The error bars in Fig. 3(A), C are within the marker sizes.

When assessing the number of adsorbed molecules, it is assumed that they are distributed uniformly over the RBC surface. Hence, fluorescence would be scattered/absorbed by the cell that would affect the recorded intensity. Namely, both excitation and emission wavelengths for FITC fit into the absorption spectrum of hemoglobin, and one could expect the dependence of the detected signal on the cell geometry. Also light scattering would result in a difference of fluorescence signals from pure dextran solution and dextran adsorbed on RBC, thus making complicated comparison of fluorophore concentration. This would result in a systematically lower signal detected from the same number of free dextran molecules in solution compared to adsorbed molecules. In the worst case (total absorption of excitation and emission signals by the cell leading to "shading" of molecules on the opposite side of the cell) this difference would be almost twofold.

3.3 Red blood cell deformability: the effect of incubation with dextran

To verify whether the observed increase in dextran adsorption onto RBC demonstrated in Fig. 2(A) is correlated to changes in the membrane properties, we performed ektacytometry experiments to measure RBC deformability caused by its incubation with dextran. Figure 4 demonstrates the dependence of the *DI* defined as $DI = (L\text{-}B) / (L + B)$, where *L* and *B* are the length and the width of the RBC as function of its incubation with dextran. Figure 4 demonstrates the dependence of the DI on shear stress for 30 and 180 minutes of incubation

Biomedical Optics EXPRESS

time in dextran solution or in PBS. It can be seen that there is no significant difference between the DI of cells incubated in dextran and of the control sample (cells incubated in PBS) at the initial stage of incubation (30 minutes). After 3 hours of incubation of RBC in dextran solution, the cells became more deformable (softer), and the DI increased by 25% compared to the control that was incubated in PBS (Fig. 4(B)).

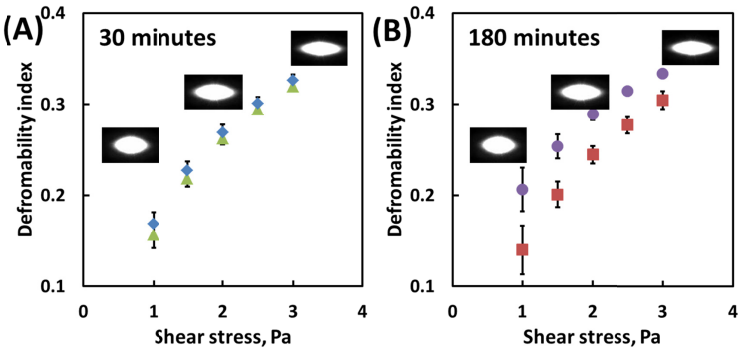

Fig. 4. The dependence of the DI on shear stress for different incubation conditions. (A) After 30 minutes of incubation either in ◆ dextran solution (dextran 70 kDa, 20 mg/ml) or in ▲ PBS. (B) After 180 minutes of incubation either in ● dextran solution or in ■ PBS. Graphs show that the *DI* becomes higher for dextran incubated cells (i.e. cells become "softer"). The insets show typical diffraction patterns obtained at different shear stresses.

4. Discussion

Joint application of optical tweezer technique combined with a microfluidic platform and fluorescence microscopy allowed us to perform semi quantitative measurements of dextran adsorption onto RBC. The obtained values of the number of adsorbed dextran molecules per cell after incubation are in good agreement with the data previously obtained by Chien et al. [6], who used radiolabeled dextran and have shown that at 20 mg/ml, RBC adsorbs approximately 90,000 of 70 kDa dextran molecules. In this work, we made use of single cell measurements and found an immediate adsorption of 20,000 FITC-labelled 70 kDa dextran molecules, accompanied by a rapid increase of the number of adsorbed molecules with incubation time, reaching ~100,000 molecules per cell after 3 hours. It is important to emphasize that our measurements are related to the amount of dextran adsorbed on a single cell after quickly (less than 1 minute) moving it from dextran solution to PBS. Due to this, the reported method is free of potential artifacts that were mentioned by some authors [17] by ensuring that the non-adsorbed macromolecules do not contribute to the signal, and the contribution of the trapped fluids is essentially absent. Non-adsorbed macromolecules are predominantly flushed away and do not contribute to the signal either, that can be controlled by the background signal in the channel with PBS. The absence of FITC label detachment from dextran was verified in control experiments. Thus, it was clearly shown that dextran adsorbs on RBC.

Our finding is of crucial importance for the assessment of the RBC interaction mechanism. The depletion theory predicts that the penetration of dextran to the glycocalyx acts as a strong inhibitor of the cells interaction [11, 22]. Thus, there should be a notable time dependent decrease in cells interaction, that can be used to evaluate the model predictions. On the other hand, our approach allows for a precise measurement of adsorbed molecules per each cell, and can be used to quantify the "bridge"-induced cells interaction. Our data can be used to establish a solid model based on the experimental evidences showing that the RBC aggregation is at least partly "bridge"-induced [7, 9, 10]. While most of the RBC 'aggregability' studies are based on dextran solutions [25], our data support the suggestion that the role of dextran is not limited solely to the depletion-inducing agent.

Biomedical Optics EXPRESS

It is also evident from the obtained results that the time-dependent change of dextran adsorption should be carefully taken into account when studying the RBC aggregation. An enhancement of dextran adsorption (Fig. 2(A)) is presumably an indication of rapid changes of membrane properties in the presence of dextran or a consequence alteration of the RBC membrane properties, occurring due to the storage. Commonly, the RBC deformability is considered to be stable for 4-8 hours of storage, followed by impaired cells properties, however, changes on shorter timescales have also been reported [19,26–32].

One of the possible reasons for RBC membrane properties alteration could be a gradual ATP-depletion, which impairs the functioning of membrane proteins, thus leading to the broken osmotic balance, as well as structural instabilities. It can be speculated that these structural instabilities could facilitate dextran attachment like in the work of Cudd et al. [13], where dextran 40 kDa covered the "holes" formed as a result of pH lowering. The penetration of dextran to these "holes" might induce further instabilities, and, as a consequence, lead to enhanced deformability and enhanced adsorption. However, understanding of the mechanisms underlying the increased dextran adsorption on RBC requires additional detailed investigation.

5. Conclusion

In the present work, we have shown that dextran adsorbs on RBC. This finding is of importance for assessing the RBC aggregation mechanisms, as for both depletion layer and bridge induced interactions, the adsorption is an important factor that has to be accounted for. We also emphasize that measurements of RBC properties should be performed with a great care, as alterations of the membrane properties are observed already after 2 hours of cells incubation *in vitro*. In general, the developed approach based on combining optical tweezers with a microfluidic platform has prospective for different applications and allows for detecting the adsorption with a high contrast at single cell level. Unlike other methods, it is possible to measure adsorption of macromolecules free of such potential artifacts as trapped fluid between cells. This approach can be used also for selecting specific cells (e.g. by age) and conditions with rapid change of the suspending media without centrifuging, thus extending the possibilities of investigation of intermolecular interactions and macromolecules adsorption.

Funding

Korean Institute for Basic Science (project code IBS-R020-D1); SonderForschungsBereich (SFB) (1027); Russian Science Foundation (grant Nº17-75-10215); Russian Foundation for Basic Research (grant Nº 16-52-51050).

Acknowledgments

The work was partially supported by Korean Institute for Basic Science (project code IBS-R020-D1). FY and CW acknowledge support from SonderForschungsBereich (SFB) (1027). The work on quantitative estimation of the number of adsorbed molecules was supported by the Russian Science Foundation (grant Nº17-75-10215). AP was supported by the Russian Foundation for Basic Research (grant Nº 16-52-51050).

Disclosures

The authors declare that there are no conflicts of interest related to this article.